10.1071/EN17150_AC

Environmental Chemistry 2018, 15(1 & 2), 58-73

Supplementary Material

On the nature of dissolved copper ligands in the early buoyant plume of hydrothermal vents

Laura Cotte[A,B,F]*, Dario Omanović*[C]*, Matthieu Waeles*[B]*, Agathe Laës*[D]*, Cécile Cathalot*[E]*, Pierre-Marie Sarradin*[A] *and Ricardo D. Riso*[B]

[A]Laboratoire Environnement Profond (LEP/EEP/REM), Ifremer, F-29280 Plouzané, France.
[B]Laboratoire des Sciences de l'Environnement Marin (LEMAR), Université de Bretagne Occidentale, F-29280 Plouzané, France.
[C]Laboratory for Physical Chemistry of Traces (LPCT), Ruđer Bošković Institute, 10002 Zagreb, Croatia.
[D]Laboratoire Détection Capteurs et Mesures (LDCM/RDT/REM), Ifremer, F-29280 Plouzané, France.
[E]Laboratoire Cycles Géochimiques et ressources (LCG/GM/REM), Ifremer, F-29280 Plouzané, France.
[F]Corresponding author. Email: cottelaura@yahoo.fr

Contents:

1. Theory

1.1. Copper complexation

In natural samples, copper (Cu) is usually found as free aqueous cation (Cu_f) and complexed by different ligands, according to the mass balance equation (1):

$$[dCu] = [Cu_f] + \sum_i [CuX_i] + \sum_i [CuL_i] \quad (1)$$

where dCu refers to the total dissolved concentration of copper in the bulk solution, $[CuX_i]$ to the concentration of Cu bound to well-defined inorganic ligands X_i (e.g. Cl^-, CO_3^{2-}, OH^-, F^-, etc.) and $[CuL_i]$ to the concentration of Cu bound to undefined ligands L_i. In seawater, the ligands L_i generally correspond to dissolved organic compounds but may also include inorganic colloids and sulfide species with high stability constants (e.g. simple $Cu(HS)^+$ and $Cu(HS)_2$ complexes or multinuclear sulfide clusters [1]).

The proportion of Cu complexed by each inorganic ligand X_i can be assessed thanks to their corresponding stability constant reported in literature (e.g.[2–4]). However, the assessment of the fraction of Cu bound to the ligands L_i is not straightforward since this fraction is an 'unlimited' mixture between simple molecules (e.g. amino acid) and more complex structures (e.g. humic substances) which are still difficult to isolate [5,6]. As each ligand from this mixture can provide several metal binding sites with specific metal-affinities [7], the usual simplification is to gather binding sites of similar complexation properties into a discrete ligand class. Each ligand class ($L_{i;\ 1<i<n}$) thus refers to a homologous ligand group of similar binding-strength. Ligand classes are ranked from the strongest, denoted as the 'L_1' ligands, to the weakest, referred to the 'L_n' ligand. It is assumed that the interaction of free Cu (Cu_f) with a specific binding-site (e.g. in the L_1 class) forms 1:1 metal-ligand complexes, as described by the equilibrium reaction (2) and the corresponding thermodynamic equilibrium stability constant (3) [8]:

$$Cu_f + L_i \xrightarrow{K_{CuL}} CuL_i \quad (2)$$

$$K_{CuL} = \frac{[CuL_i]}{[Cu_f][L_i]} \quad (3)$$

The charges of the different species involved are omitted to simplify. Note that considering only that particular equilibrium is an ideal case where there are only these two species (Cu_f and L_i) in the bulk solution. In practice, both are involved in numerous competing side reactions depending on the sample composition. The stability constant K_{CuL} has therefore to be adapted according to the experimental conditions (pH, major ion composition, etc.) to reflect as best as possible the stability of the complex of interest (CuL_i) [9]. Side reactions involving the ligands X_i are fully identified as major ion composition and pH are well known in seawater [10] and can be summarized by the chemical equilibrium (4), where $[X_i']$ refer to the concentration of unbound ligands:

$$Cu_f + X_i' \xrightarrow{K_{CuX}} CuX_i \quad (4)$$

Side reactions for L_i are predominantly interactions between protons and other competing cations such as Ca^{2+} and Mg^{2+} with the ligand of interest. As the degrees of protonization and of complexation are not known in seawater, it is not possible to correct the thermodynamic stability constant K_{CuL} for such side reactions [10]. The use of the so-called 'conditional stability constant' K'_{CuL} which takes into account all interfering side reactions is therefore favored (5):

$$K'_{CuL} = \frac{[CuL_i]}{[Cu'][L'_i]} \quad (5)$$

where $[Cu']$ refers to the sum of the concentrations of free copper ions (Cu_f) and of copper bound to other compounds than the ligand (L_i) (6):

$$[Cu'] = [Cu_f] + [CuX_i] \quad (6)$$

and where $[L'_i]$ denotes the total concentration of the ligand targeted not bound to copper. This includes the concentration of the protonated ligand $[LH_i]$, the free ligand concentration $[L_{i_f}]$, as well as the concentration of the complexes of L_i with other ambient cations (M_j) (7):

$$[L'_i] = [L_{i_f}] + [LH_i] + \sum [M_j L_i] \quad (7)$$

K'_{CuL} is therefore unique to each solution considered.

1.2. Titration of natural binding ligands

The quantitative analysis of natural ligands L_i requires techniques that need to be sensitive enough and highly selective such as the competitive ligand exchange - adsorptive cathodic stripping voltammetry (CLE-AdCSV) [10]. The CLE-AdCSV relies on a competitive exchange of the target metal between natural ligands L_i and a well-known added ligand. Here, salicylaldoxime (SA) was selected as the added ligand [11] to perform the complexometric Cu-ligand titrations. The SA added (in excess) is usually assumed to form two electroactive complexes, i.e. $Cu(SA)_x$ (x = 1 or 2), according to the chemical equilibrium (8) and (9):

$$Cu_f + SA \xrightarrow{K'_{Cu(SA)}} Cu(SA) \quad (8)$$

$$Cu_f + 2SA \xrightarrow{\beta'_{Cu(SA)2}} Cu(SA)_2 \quad (9)$$

where $K'_{Cu(SA)}$ and $\beta'_{Cu(SA)2}$ are the conditional stability constants for $Cu(SA)$ and $Cu(SA)_2$, respectively. They are both described according to the equations (10) and (11), respectively.

$$K'_{Cu(SA)} = \frac{[Cu(SA)]}{[Cu_f][SA']} \quad (10)$$

$$\beta'_{Cu(SA)2} = \frac{[Cu(SA)_2]}{[Cu_f][SA']^2} \quad (11)$$

These two parameters depend on the sample composition because of the ability of SA to react with other metal such as Fe [12,13]. The addition of SA is then followed by additions of progressively increasing concentrations of Cu to titrate the natural ligands L_i in solution. Once full equilibrium is reached, the $Cu(SA)_x$ complexes are adsorbed to the mercury drop electrode by application of a defined potential and then stripped from the drop. The current measured from the stripping step corresponds to the reduction of the accumulated complexes (from Cu(II) to Cu(0)) and is proportional to the quantity of $Cu(SA)_x$ adsorbed to the drop, itself proportional

to the concentration of $Cu(SA)_x$ in the bulk solution. The addition of SA in excess changes the natural mass balance equation which has to be reconsidered as follows (12):

$$[dCu] = [Cu_f] + \sum_i [CuX_i] + \sum_i [CuL_i] + [Cu(SA)_x] \quad (12)$$

The total concentration of the $[Cu(SA)_x]_T$ complexes is then inferred by combining equations (10) and (11) as follows (13):

$$[Cu(SA)_x]_T = [Cu_f]\left(K'_{CuSA}.[SA] + \beta'_{Cu(SA)2}.[SA]^2\right) \quad (13)$$

The conditional stability constants K'_{CuSA} and $\beta'_{Cu(SA)2}$ are calculated and adapted according to salinity using the two empirical relationships provided by Campos & van den Berg [11]. The amount of the non-electroactive CuL_i species and, thereafter, the complexing parameters of the ligand of interest (L_i) can finally be inferred using equation (12).

1.3. Side reaction coefficient

Side reaction coefficients (SRC) reflect the combined effect of all side reactions occurring between Cu and the other ligands in the bulk solution, i.e. X_i or L_i ligands. They express the competitive strength of each type of ligand for Cu and are equivalent to the concentration ratio of complexed to free Cu ion as shown in equations (14) and (15) [8]:

$$\alpha_L = \frac{[CuL_i]}{[Cu_f]} = K_i'.[L_i'] \quad (14)$$

$$\alpha_X = \frac{[Cu']}{[Cu_f]} = \frac{[CuX_i] + [Cu_f]}{[Cu_f]} = K_i'.[X_i'] \quad (15)$$

Where α_L and α_X refer to the SRCs in which Cu is involved with L_i and X_i, respectively. In the case of the AdCSV method, the SRC related to the complexation of labile Cu by the added SA ($\alpha_{Cu(SA)x}$) has to be taken into account and the CuX_i species are assumed to be negligible when compared to the excess of SA added. Knowing the given conditional stability constants K'_{CuSA}

and $\beta'_{Cu(SA)2}$, the SRCα_{SA} is inferred from the equation (13) which can be rewritten as follows (16):

$$\alpha_{Cu(SA)x} = K'_{CuSA}.[SA'] + \beta'_{Cu(SA)2}.[SA']^2 \quad (16)$$

Combing equations (10), (11) and (16) leads to the simpler relationship for the assessment of $[Cu(SA)_x]_T$ (17):

$$[Cu(SA)_x]_T = \alpha_{Cu(SA)}.[Cu_f] \quad (17)$$

The final fitting of the obtained experimental data to mathematical model (see below) will be therefore less complicated, whatever the calculation procedure used.

1.4. Calculation of the complexing capacity

The current (I_P) measured during the stripping step is proportional to the total concentration of the $Cu(SA)_x$ complexes in the bulk solution and to the corresponding sensitivity S of the analytical method used (18):

$$I_P = S.[Cu(SA)_x]_T \quad (18)$$

And thus combining equations (17) and (18):

$$I_P = S.\alpha_{Cu(SA)}.[Cu_f] \quad (19)$$

Knowing $\alpha_{Cu(SA)}$, I_P and S, the concentration of free copper $[Cu_f]$ can be calculated from equation (19), enabling then the determination of $[CuL_i]$ and, finally, the assessment of the complexation parameters [9].

The complexing parameters K'_{CuL} and $[L'_i]$ need further well-established mathematical transformations to be estimated. In the case where only one ligand class is detected, the Ružić/van den Berg [10,14] and the Scatchard [15] linearizations methods are generally used and expressed by the equations (20) and (21), respectively. Both resulting plots provide a linear relationship from which the two parameters are deduced.

$$\frac{[Cu_f]}{[CuL_i]} = \frac{[Cu_f]}{[L'_i]} + \frac{1 + \alpha_{Cu(SA)}}{[L'_i].K'_{CuL}} \quad (20)$$

By plotting $[Cu_f]/[CuL_i]$ against $[Cu_f]$, $[L'_i]$ is indeed determined from the inverse of the slope of the linear regression and K_{CuL} is obtained from the inverse of the x-axis intercept.

$$\frac{[CuL_i]}{[Cu_f]} = -K'_{CuL}.[CuL_i] + K'_{CuL}.[L'_i] \quad (21)$$

The Scatchard transformation requires to plot $[CuL_i]/[Cu_f]$ versus $[CuL_i]$ to estimate L'_i and K'_{CuL}. When two or more ligand classes are present, these mathematical transformations provide a curvature shape of the final plot. The Ružić/van den Berg transformation could be extended to a multi-ligand system [16] but not the Scatchard method [17]. In that case, a non-linear regression such as the Langmuir/Gerringa technique [18] is recommended to better fit the experimental titration curve and to provide correct estimate of L'_i and K'_{CuL} corresponding to each class detected. The non-linear Gerringa method is shown in equation (22) and can be extended to a multi-ligand system:

$$[CuL_i] = \frac{K'_{CuL}[Cu_f][L'_i]}{1 + K'_{CuL}[Cu_f]} \quad (22)$$

The plot of $[CuL_i]$ versus $[Cu_f]$ is used to fit the experimental titration curves.

For a multi-ligand system, a mathematical software is needed to perform the non-linear fitting. Above described approaches are based on analytical solutions, however, a methodology based on solving the true mass-balance equilibria of all components included in the system was developed and recommended for the CLE-AdCSV technique [8,17,19–22]. A particular advantage of this approach is its ability to process experimental data obtained at different 'detection windows' as an unified set of data, leading to a reliable estimation of complexation parameters [8,19,21,22]. In the present study, the software ProMCC [17] was used to fit the experimental data. ProMCC includes both analytical solutions and the mass balance equilibrium approach. The mass balance equilibrium approach, referred as 'complete complexation fitting model' in ProMCC was used for all calculations.

For all samples, the use of 1 ligand model gave proper estimations of both conditional stability constant and Cu-binding ligands concentrations. It should be noted that, in few cases, the Ruzic-van den Berg and Scatchard linearization plots gave indication of the presence of two ligand classes. However, the deviation from the linearity was caused mostly by the first three points of the titration curves. In these cases, unusually high stability constants with huge uncertainties were obtained for the first ligand. Such cases are considered as unrealistic and the "outlier" points were discarded in the treatment by using a one-ligand model.

2. Desorption step procedure

The potential jump enables the reduction/dissolution of the HgS layer according to equation (1). A drastic decrease of the HgS interference (e.g. 20 fold lower for 09632 C3, not shown) as well as a better defined and reversible $Cu(SA)_x$ signal were obtained thanks to the desorption step (DS). The two (or more) superimposed reduction peaks at -0.01 V (Figure 3) completely disappeared too, suggesting a possible link with the RSS species. Overall, the shape of all voltammograms was improved through this step, as their final appearance was the same than those obtained for untreated samples, without addition of Cu. The linearity in response to the increasing additions of Cu needed then to be tested using the adapted procedure. The adapted procedure well succeeded under laboratory conditions (i.e. UVSW spiked with the artificial ligand DTPA (10 nM) and SA (4 μM), pH 8.2) with similar sensitivity than for the classical method. However, it failed when performed on samples because of a great loss of linearity with increasing addition of Cu. Thus, titration experiments on pretreated samples were carried out using the classical procedure (no DS), despite the encountered problems.

Table S1. End-member concentrations in the fluids sampled at Lucky Strike (extrapolated to Mg-zero) from T. Leleu PhD thesis 2017 and V. Chavagnac (GET, CNRS) and in deep seawater.

Location	T	dMn	Cl-
2015	°C	µM	mM
Aisics	307	257	428
Y3	326	280	578
Seawater	4	0.002	546

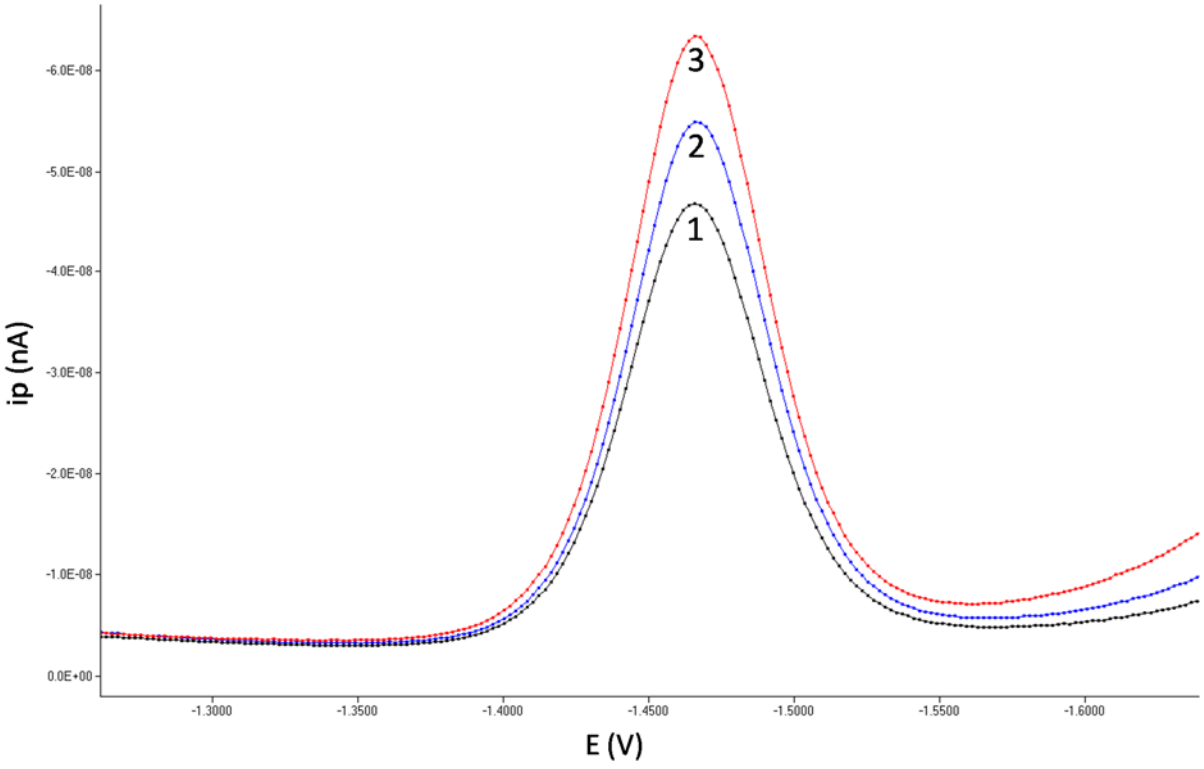

Figure S1. Reduction peak of Mn(II) for sample 02598 C1: (1) before addition of Mn^{2+} and after addition of (2) 5 and (3) 15 µM Mn^{2+}.

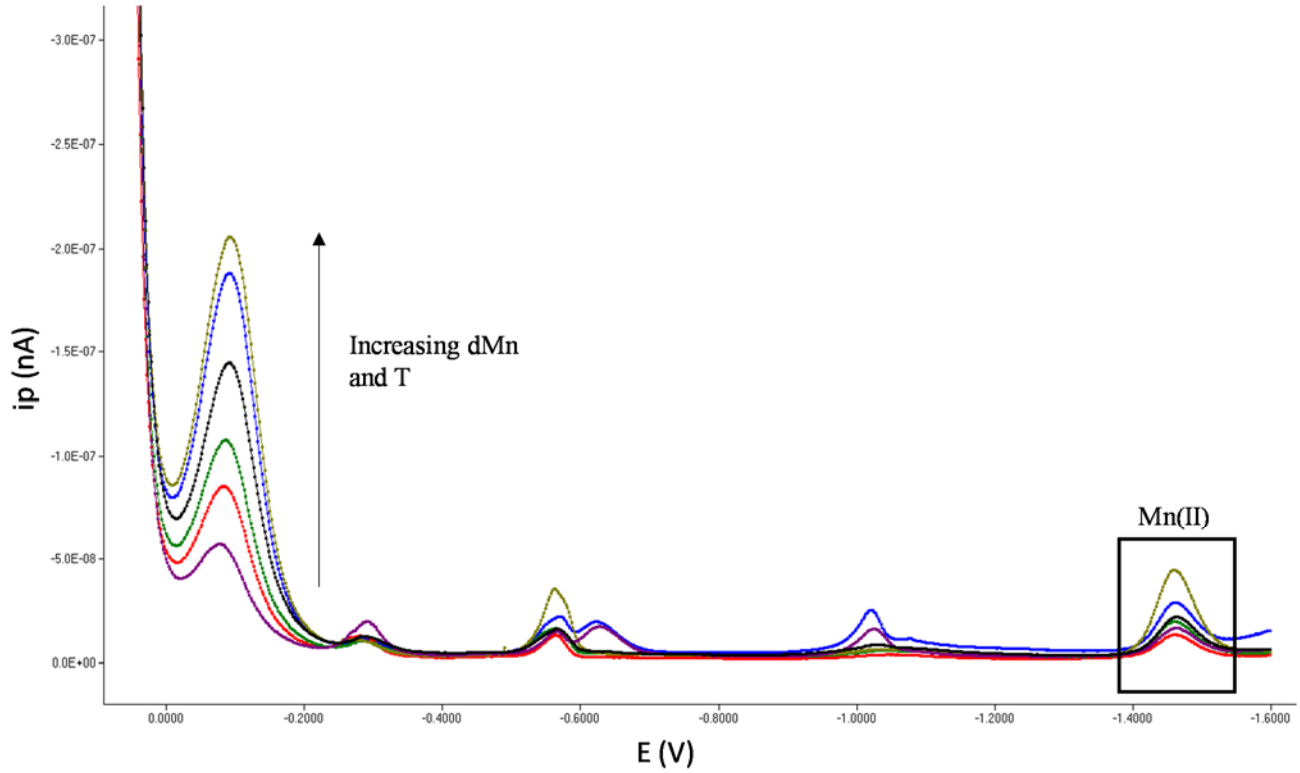

Figure S2. Shape of the voltammograms (without additions of Cu) when getting closer to the vent orifice for dive 02598 (by ascending order the signal corresponds to E3, C3, D2, B3, C1 and E1; deposition time 60 s).

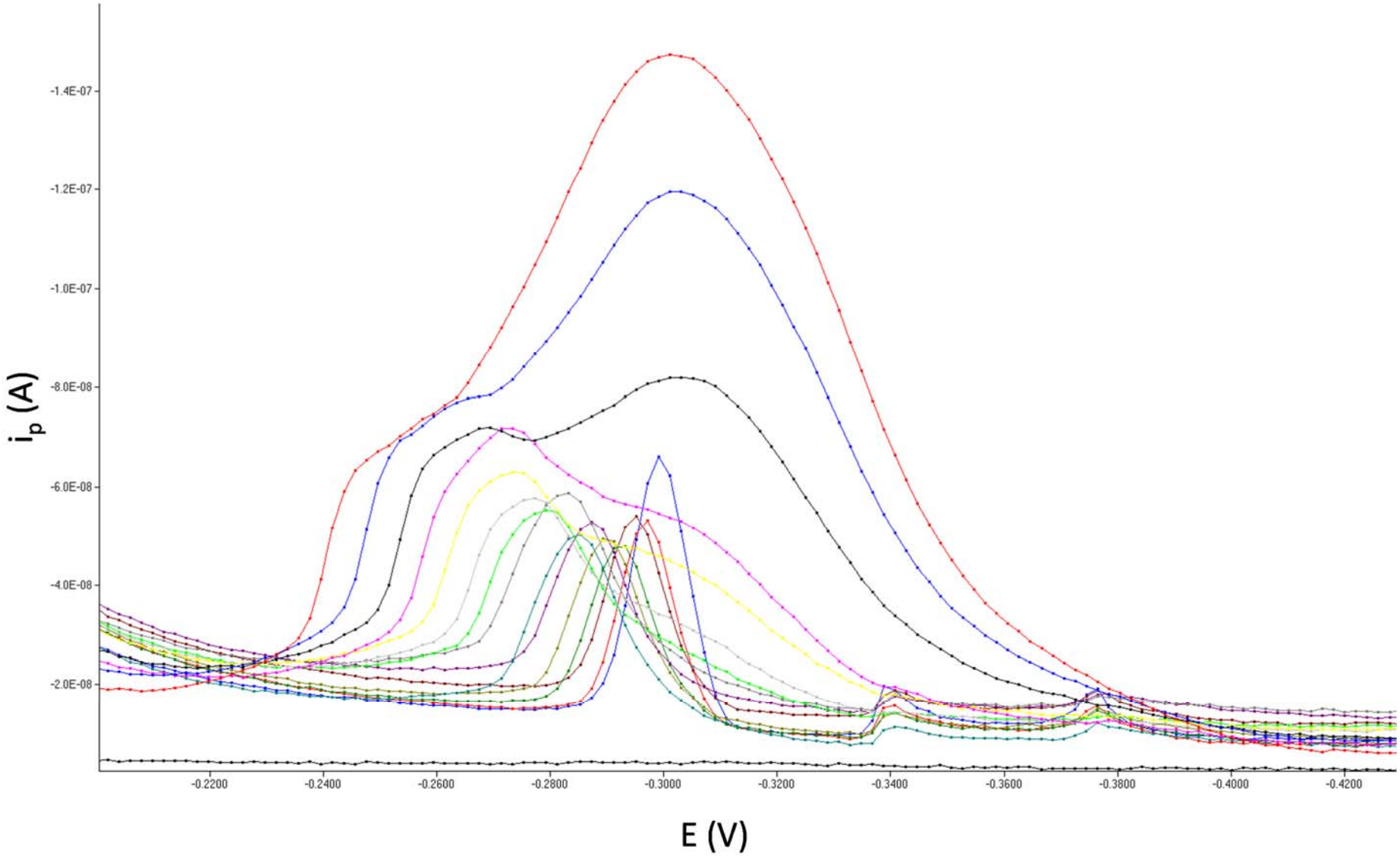

Figure S3. $Cu(SA)_x$ signals obtained for the pre-treated samples. The plot corresponds to the inset of Figure 3B but with the potential scale provided.

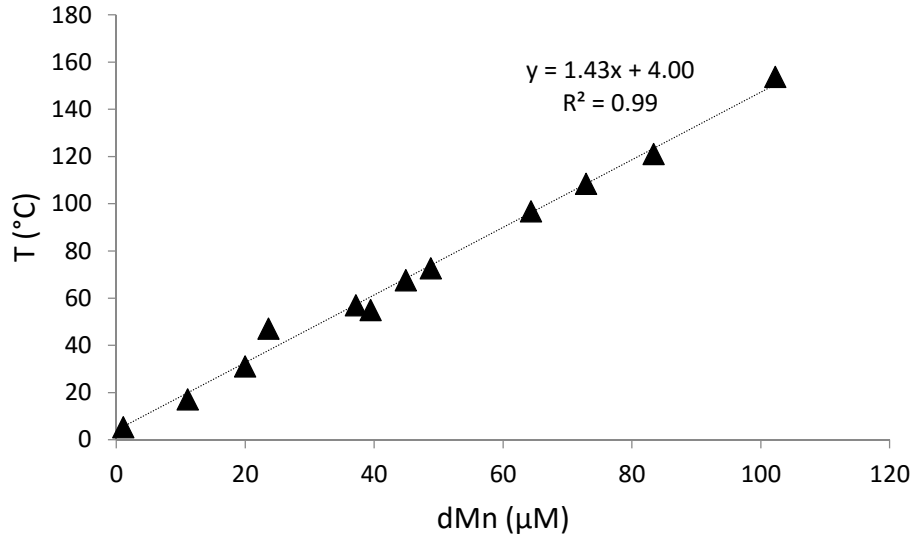

Figure S4. dMn-T relationship obtained at Aisics (dive 02598, 2015) with the PEPITO sampler. The linear regression is used so that the ΣS concentrations can be plotted as a function of their corresponding dMn (if T_{PEPITO} and $T_{CHEMINI}$ are different).

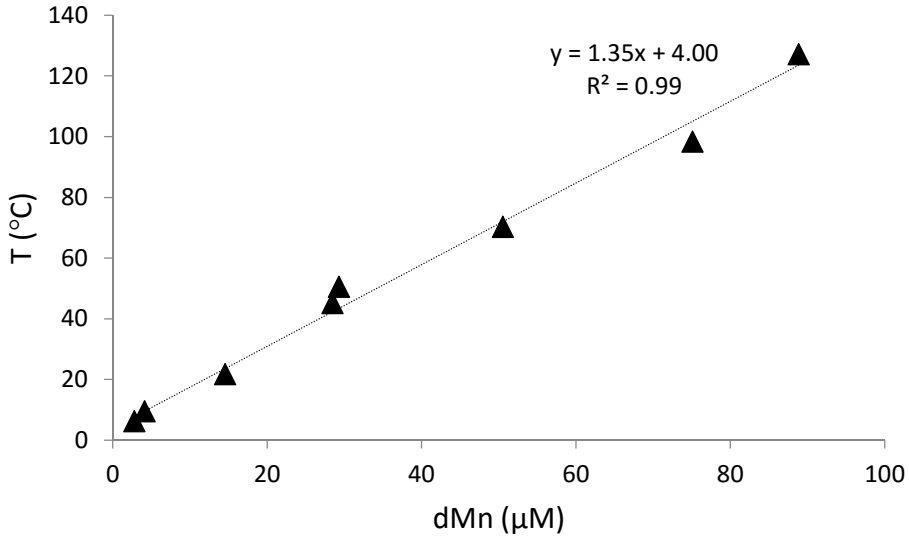

Figure S5. dMn-T relationship obtained at Y3 (dive 07582, 2014) with the PEPITO sampler.

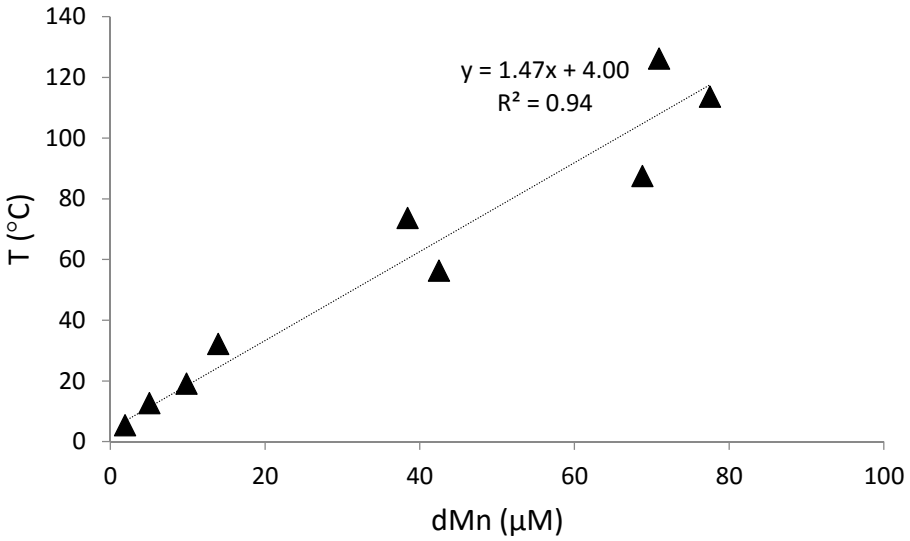

Figure S6. dMn-T relationship obtained at Aisics (dive 09632, 2016) with the PEPITO sampler.

References

[1] T.F. Rozan, M.E. Lassman, D.P. Ridge, G.W. Luther, Evidence for iron, copper and zinc complexation as multinuclear sulphide clusters in oxic rivers, *Nature* **2000**, *406*, 879–882. doi:10.1038/35022561.

[2] D.R. Turner, M. Whitfield, A.G. Dickson, The equilibrium speciation of dissolved components in freshwater and sea water at 25°C and 1 atm pressure, *Geochimica et Cosmochimica Acta* **1981**, *45*, 855–881. doi:10.1016/0016-7037(81)90115-0.

[3] R.H. Byrne, L.R. Kump, K.J. Cantrell, The influence of temperature and pH on trace metal speciation in seawater, *Marine Chemistry* **1988**, *25*, 163–181. doi:10.1016/0304-4203(88)90062-X.

[4] D. Turner, E.P. Achterberg, C.-T.A. Chen, S. Clegg, V. Hatje, M. Maldonado, S.G. Sander, C.M.G. van den Berg, M. Wells, Towards a quality-controlled and accessible Pitzer model for seawater and related systems, *Frontiers in Marine Science* **2016**, *3*, 1–21.

[5] J. Buffle, Complexation reactions in aquatic systems: An analytical approach, *John Wiley and Sons* **1988**.

[6] M. Filella, Freshwaters: which NOM matters?, *Environmental Chemistry Letters* **2009**, *7*, 21–35. doi:10.1007/s10311-008-0158-x.

[7] D.A. Dzombak, W. Fish, F.M. Morel, Metal-humate interactions. 1. Discrete ligand and continuous distribution models., *Environmental Science & Technology* **1986**, *20*, 669–675.

[8] I. Pižeta, S.G. Sander, R.J.M. Hudson, D. Omanović, O. Baars, K.A. Barbeau, K.N. Buck, R.M. Bundy, G. Carrasco, P.L. Croot, C. Garnier, L.J.A. Gerringa, M. Gledhill, K. Hirose, Y. Kondo, L.M. Laglera, J. Nuester, M.J.A. Rijkenberg, S. Takeda, B.S. Twining, M. Wells, Interpretation of complexometric titration data: An intercomparison of methods for estimating models of trace metal complexation by natural organic ligands, *Marine Chemistry* **2015**, *173*, 3–24. doi:10.1016/j.marchem.2015.03.006.

[9] Z.D. Powell, Voltammetric studies on the stabilisation of dissolved copper in hydrothermal vent fluids, *PhD Thesis, University of Otago, Dunedin, New Zealand* **2014**.

[10] C.M.G. van den Berg, Determination of copper complexation with natural organic ligands in seawater by equilibration with MnO2 I. Theory, *Marine Chemistry* **1982**, *11*, 307–322. doi:10.1016/0304-4203(82)90028-7.

[11] M.L.A.M. Campos, C.M.G. van den Berg, Determination of copper complexation in sea water by cathodic stripping voltammetry and ligand competition with salicylaldoxime, *Analytica Chimica Acta* **1994**, *284*, 481–496. doi:10.1016/0003-2670(94)85055-0.

[12] M.M. Abualhaija, C.M.G. van den Berg, Chemical speciation of iron in seawater using catalytic cathodic stripping voltammetry with ligand competition against salicylaldoxime, *Marine Chemistry* **2014**, *164*, 60–74. doi:10.1016/j.marchem.2014.06.005.

[13] C. Kleint, J.A. Hawkes, S.G. Sander, A. Koschinsky, Voltammetric investigation of hydrothermal iron speciation, *Frontiers in Marine Science* **2016**, *3*, 75. doi:10.3389/fmars.2016.00075.

[14] I. Ružić, Theoretical aspects of the direct titration of natural waters and its information yield for trace metal speciation, *Analytica Chimica Acta* **1982**, *140*, 99–113. doi:10.1016/S0003-2670(01)95456-X.

[15] G. Scatchard, The attractions of proteins for small molecules and ions, *Annals of the New York Academy of Sciences* **1949**, *51*, 660–672.

[16] K.W. Bruland, E.L. Rue, J.R. Donat, S.A. Skrabal, J.W. Moffett, Intercomparison of voltammetric techniques to determine the chemical speciation of dissolved copper in a coastal seawater sample, *Analytica Chimica Acta* **2000**, *405*, 99–113. doi:10.1016/S0003-2670(99)00675-3.

[17] D. Omanović, C. Garnier, I. Pižeta, ProMCC: An all-in-one tool for trace metal complexation studies, *Marine Chemistry* **2015**, *173*, 25–39. doi:10.1016/j.marchem.2014.10.011.
[18] L.J.A. Gerringa, P.M.J. Herman, T.C.W. Poortvliet, Comparison of the linear van den Berg/Ružić transformation and a non-linear fit of the Langmuir isotherm applied to Cu speciation data in the estuarine environment, *Marine Chemistry* **1995**, *48*, 131–142. doi:10.1016/0304-4203(94)00041-B.
[19] R.J. Hudson, E.L. Rue, K.W. Bruland, Modeling complexometric titrations of natural water samples, *Environmental Science & Technology* **2003**, *37*, 1553–1562.
[20] C. Garnier, I. Pižeta, S. Mounier, J.Y. Benaïm, M. Branica, Influence of the type of titration and of data treatment methods on metal complexing parameters determination of single and multi-ligand systems measured by stripping voltammetry, *Analytica Chimica Acta* **2004**, *505*, 263–275. doi:10.1016/j.aca.2003.10.066.
[21] S.G. Sander, K.A. Hunter, H. Harms, M. Wells, Numerical approach to speciation and estimation of parameters used in modeling trace metal bioavailability, *Environmental Science & Technology* **2011**, *45*, 6388–6395.
[22] M. Wells, K.N. Buck, S.G. Sander, New approach to analysis of voltammetric ligand titration data improves understanding of metal speciation in natural waters, *Limnology and Oceanograhy: Methods* **2013**, *11*, 450–465.